This order is generally that expected from the trends obtained from CO stretching frequencies in L-substituted carbonyl complexes. The position of the isonitrile is not accurately determined because of the overlapping of the absorption bands. It can only be concluded that the π-acceptor abilities are similar to those of the carbonyl ligand. It is a better π acceptor than any of the other ligands in Figure 5.

The position of the halides in the π series, taken at face value, is unexpected. They appear to be weaker π donors than expected. We and others have pointed out that the π parameter, which ultimately is traced back to the d_{xy}, d_{xz}, and d_{yz} orbital energies, is influenced by electrostatic interactions with ligand σ-donor orbital's lone pair of electrons.[18,26,27] Thus in the square-planar complexes, both the d_{xy} and the d_{xz} orbitals are raised in energy by the electrostatic interaction with a strong σ-donor ligand L, and vice versa. This type of interaction should be particularly evident when the e_σ values are very large as is the case for NMe_3 and PEt_3 and of correspondingly less importance when the e_σ values are relatively small as is the case for Cl^- and Br^-. A useful interpretation of the π-interaction properties can be obtained by considering the value of the AOM π parameter relative to that of the σ parameter, i.e., the value of e_π/e_σ.

When the ligands in Figure 5 are ordered in terms of this normalized π parameter, the order in terms of increasing π-acceptor (decreasing π donor) ability is $Cl = Br < NMe_3 < PEt_3 < PPh_3 < AsPh_3 < C_2H_4 < CNC(CH_3)_3 = CO$. This normalized series does not affect the relative positions of the strong π-acceptor ligands but does place the halides as poorer π acceptors than the ammine, the position it occupies in the high oxidation state "Werner" complexes.

Conclusions

The single-crystal polarized electronic absorption spectra of $(Pr_4N)[PtCl_3CO]$, $(Pr_4N)[PtBr_3CO]$, and $(Pr_4N)[PtCl_3CNC(CH_3)_3]$ have been obtained and assigned. The metal-carbonyl bond is strongly weakened in the excited state. A Franck-Condon analysis of the vibronic structure shows that the Pt-C bond is lengthened by 0.18 Å. The stretching frequency decreased by about 100 cm^{-1}. The σ and π interactions of carbon monoxide with a metal are determined for the first time from electronic spectroscopy and ligand-field theory. Carbon monoxide is a very strong π-acceptor ligand as expected. It is a surprisingly strong σ-donor ligand. It's σ interaction with the metal is larger than that of chloride and bromide and about equal to that of ethylene. It is a much weaker σ donor than phosphines or ammines. Its position in the two-dimensional spectrochemical series is shown in Figure 5.

Acknowledgment. The support of this research by the National Science Foundation is gratefully acknowledged.

(26) Byrn, M. P.; Katz, B. A.; Keder, N. L.; Levan, K. R.; Magurany, C. J.; Miller, K. M.; Pritt, J. W.; Strouse, C. E. *J. Am. Chem. Soc.* **1983**, *105*, 4916.
(27) Keeton, M.; Chou, B. F.; Lever, A. B. P. *Can. J. Chem.* **1971**, *49*, 192.

On the Mechanism of Stereoselective Epoxidation of Alkenes by Oxo-Iron Porphyrins

Karl Anker Jørgensen

Contribution from the Department of Organic Chemistry, Chemical Institute, Aarhus University, DK-8000 Aarhus C, Denmark. *Received March 12, 1986*

Abstract: The structure of oxo-iron porphyrins and their stereoselective epoxidation properties of alkenes are analyzed from a theoretical point of view. It is found that the most stable structure of oxo-iron porphyrin is one in which oxygen is inserted into the iron-nitrogen bond. This structure is equivalent to some of the carbene analogues, and the bond lengths for Fe-O (1.9 Å) and N-O (1.4 Å) are in good agreement with those found in the nickel analogue of **6**. The insertion of oxygen into the iron-nitrogen bond makes some of the d orbitals on iron available for interaction with the alkene; this type of complex is supported by recent experimental observations. The alkene can be coordinated in a perpendicular or parallel orientation at the iron atom (relative to the iron-oxygen bond), and the perpendicular orientation is found to be the most favorable. This binding of the alkene can then cause the stereoselective epoxidation properties, as the trans substituents will interact repulsively with the iron-porphyrin moiety. It is then suggested that the next step in the reaction mechanism is a slipping motion of the alkene toward the oxygen. This motion is controlled by a favorable interaction between the π^* orbital of the alkene and the lone pair on the oxygen which is antisymmetric with respect to the iron-oxygen-nitrogen plane. Aspects of this type of mechanism in relation to the experimental results as well as other transition metal catalyzed epoxidation reactions are discussed.

Iron functions as the principal electron carrier in biological oxidation-reduction reactions.[1] Iron also serves to transport and store molecular oxygen, a function that is essential to the life of all vertebrates.[1] As to the structure of the oxygen-iron bond in hemoglobin, Collman's group has found that oxygen binds in an end-on fashion (Pauling's model) to the iron of the protoheme, rather than in the sideways manner proposed by some theories.[2] Removal of an oxygen atom from hemoglobin leads to an oxo-iron(V) porphyrin, generally written as **1** (the hydrogen atoms are omitted for clarity), which is now generally accepted to be the active oxidant in P-450 monooxygenase, catalase, peroxidase,

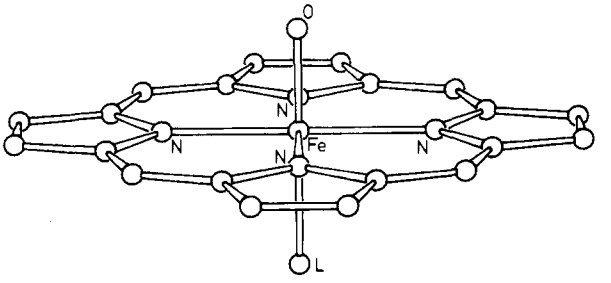

1

and chloroperoxidase.[3] **1** has also been shown to be a useful catalyst in oxidation reactions in organic synthesis.[4]

(1) See, e.g.: Dugas, H.; Penney, C. *Bioorganic Chemistry*; Springer-Verlag: New York, 1981; pp 346-362 and reference related to these pages.
(2) Collman, J. P. *Acc. Chem. Res.* **1977**, *10*, 265-272.

0002-7863/87/1509-0698$01.50/0

Scheme I

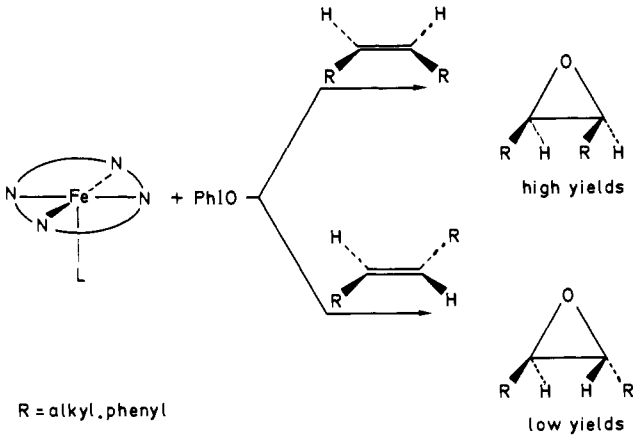

Oxo-iron porphyrins, **1**, are able to hydroxylate an unactivated C–H bond in an alkane to the corresponding alcohol and to oxidize a primary alcohol to an aldehyde.[3] Another important property of **1** is its ability to epoxidize alkenes, and the stereospecific epoxidation observed with some oxo-iron porphyrins has been an especially attractive area.[3,4] Cis alkenes are transformed to cis epoxides in high yields, whereas trans alkenes give low yields of trans epoxides using **1** (generated from, e.g., tetraphenylporphinatoiron(III) chloride and iodosylbenzene);[4] see Scheme I.

The mechanism for the stereoselective oxygen transfer from **1** to the carbon–carbon double bond is not very well understood and has been discussed in a series of papers[4] as well as in books.[1,2] Several reasonable geometries for the approach of the alkene to the oxo-iron group have been suggested,[4c,d] and some of them are depicted in **2**–**4**.

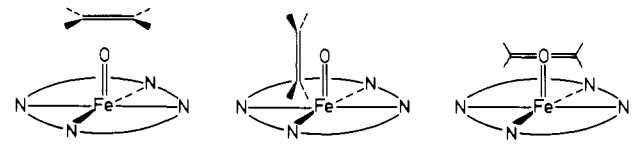

2 3 4

Approach as in **2** along the axis of Fe–O bond is unlikely to be involved here, as no preference of cis rather than trans alkenes should then be observed. Geometry **3** should be particularly favorable for 1,1-disubstituted alkenes. This type of mechanism has been suggested by Sharpless et al.[5] for the alkene epoxidation by chromyl chloride with the metallacycle **5** as intermediate.

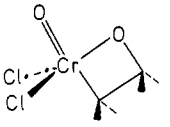

5

Metallacycle **5** received later support by GVB molecular orbital calculations performed by Goddard et al.[6] This type of mechanism is also unlikely to be involved in the stereoselective epoxidation of alkenes by oxo-iron porphyrins as both cis and trans alkenes should be very unreactive because of the steric repulsion between the substituents in the alkene and the porphyrin ring. Furthermore, it has been observed that methylenecyclohexane reacts much more slowly than cycloheptene,[4c] which also argues against geometry **3**. Mechanism **4**, which is an approach of the double bond from the side and parallel to the plane of the porphyrin ring, does to some extent explain the stereoselective epoxidation properties of **1**. But why should mechanism **4** be more favorable than **2**? In both cases the primary interaction leading to the epoxide probably occurs between electron(s) located at the oxygen in **1**, antisymmetric with respect to the N–Fe–N plane, and the antisymmetric π^* orbital of the alkene. From this molecular orbital point of view one should thus expect mechanism **4** to be equal to mechanism **2**, and it is thus not quite obvious what should cause an alkene to approach as in mechanism **4**.

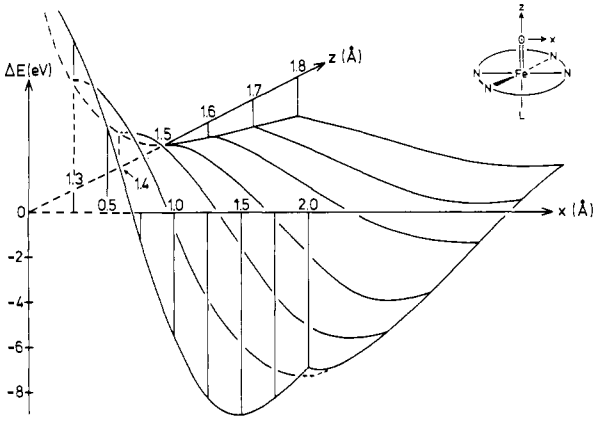

Figure 1. The change in total energy of the oxo-iron porphyrin system as a function of the slipping motion of oxygen as indicated in the upper right corner. The energy zero is taken to be the symmetric form $x = 0$ Å and $z = 1.5$ Å.

The primary goal with this paper is to present a coherent theoretical model that allows one to understand the observed stereoselective reactivity and intermediates. For these purposes symmetry arguments and transition-metal INDO,[7] CNDO,[7] and extended Hückel[8] calculations are used.

Structure of Oxo-Iron Porphyrins

In attempting to understand the stereoselectivity of oxo-iron porphyrins we will start with the structure of these types of systems. Besides the high-symmetry structure of oxo-iron porphyrins like the one shown as **1**, Tatsumi and Hoffmann,[9] as well as others,[10] have recently pointed out that several other structures of oxo-iron porphyrin might be possible such as those shown in **6** and **7** (hydrogen atoms are omitted for clarity).

Oxo-iron porphyrins are very unstable and highly reactive species, though they have been detected spectroscopically at low temperatures.[4d,11] In light of the X-ray structures of the carbene analogue[12] of **6**, where the carbene group is inserted into the iron–nitrogen bond, and the nickel analogue[13] of **6**, this type of

(3) See, e.g.: (a) Sheldon, R. A.; Kochi, J. K. *Metal-Catalyzed Oxidations of Organic Compounds*; Academic Press: New York, 1981; pp 245–268 and references therein. (b) Nappa, M. J.; Tolman, C. A. *Inorg. Chem.* **1985**, *24*, 4711 and references therein. (c) Ulrich, V. *Top. Curr. Chem.* **1984**, *121*, 68.

(4) See, e.g.: (a) Baldwin, J. E; Perlmutter, L. *Top. Curr. Chem.* **1984**, *121*, 182–220. (b) Patin, M.; Mignani, C. *J. Chem. Soc., Chem. Commun.* **1979**, 685. (c) Groves, J. T.; Nemo, T. E. *J. Am. Soc.* **1983**, *105*, 5786, 5791, 6243. (d) Groves, J. T. *J. Chem. Educ.* **1985**, *62*, 928 and references therein. (e) Dicken, C. M.; Lu, F.-L.; Nee, M. W.; Bruice, T. C. *J. Am. Chem. Soc.*, **1985**, *107*, 5776. (f) Smidt, J. R. L.; Sleath, P. R. *J. Chem. Soc., Perkin Trans. 2* **1982**, 1009. (g) Guemgerich, F. P.; McDonald, T. L. *Acc. Chem. Res.* **1984**, *17*, 9.

(5) Sharpless, K. B.; Teranishi, A. Y.; Bäckvall, J. E. *J. Am. Chem. Soc.* **1977**, *99*, 3120.

(6) Rappé A. K.; Goddard, W. A., III *J. Am. Chem. Soc.* **1980**, *102*, 5114; *Nature (London)* **1980**, *285*, 311.

(7) (a) Pople, J. A.; Beveridge, D. L. *Approximate Molecular Orbital Theory*; McGraw-Hill: New York, 1970. (b) Bacon, A. D.; Zerner, M. C. *Theor. Chim. Acta* **1979**, *53*, 21 and references therein.

(8) (a) Hoffmann, R. *J. Chem. Phys.* **1963**, *39*, 1397. (b) Hoffmann, R.; Lipscomb, W. N. *Ibid.* **1962**, *36*, 2179; **1962**, *37*, 2872.

(9) Tatsumi, K.; Hoffmann, R. *Inorg. Chem.* **1981**, *20*, 3771.

(10) (a) Strich, A.; Veillard, A. *Nouv. J. Chim.*, **1983**, *7*, 347. (b) Jørgensen, K. A. *Acta Chem. Scand., Ser. B* **1986**, *40*, 512.

(11) (a) Chim. D.-H.; Balch, A. L.; La Mar, G. N. *J. Am. Chem. Soc.* **1980**, *102*, 1446. (b) Chim., D.-H.; La Mar, G. N.; Balch, A. L. *Ibid.* **1980**, *102*, 4344.

(12) (a) Chevrier, B.; Weiss, R.; Lange, M.; Chottard, J.-C.; Mansuy, D. *J. Am. Chem. Soc.* **1981**, *103*, 2899. (b) Latos-Grazynski, L.; Cheng, R.-J.; La Mar, G. N.; Balch, A. L. *Ibid.* **1981**, *103*, 4270.

(13) Bach, A. L.; Chan, Y.-W.; Ohnstead, M. O. *J. Am. Chem. Soc.* **1985**, *107*, 6510.

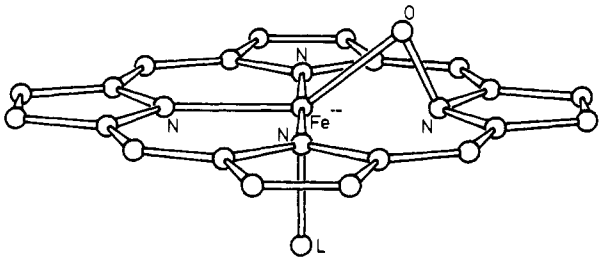

6

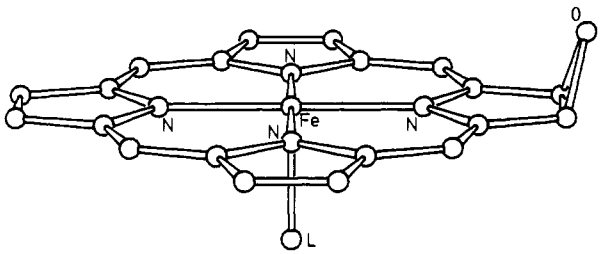

7

structure of oxo-iron porphyrin appears worth considering.

Figure 1 shows the calculated INDO total energy surface as a function of the slipping displacements of oxygen toward nitrogen (x axis) and the distance between oxygen and the iron porphyrin plane (z axis). It appears from Figure 1 that the oxo-iron porphyrin system is stabilized when the oxygen moves toward nitrogen, and the energy minimum for the system is found in a region where the oxygen is about 1.2 Å from the iron porphyrin plane and 1.5 Å out along the x axis. This structure corresponds to the one shown as **6**. From the results in Figure 1 the stabilization of **6** relative to **1** is about 8 eV (~180 kcal).[14] The bond lengths for Fe–O (~1.9 Å) and N–O (~1.4 Å) are in good agreement with those found in the nickel analogue of **6**.[13] CNDO calculations give a nearly similar energy surface. It should be noted that the total energy increases for the system for $x = 0$ and $z > 1.85$ Å.

The observed instability of the near "near C_{4v}" structure **1** relative to **6** can be traced to the frontier orbitals of the system. The INDO calculations give the three Fe d orbitals xy, xz, and yz low in energy and $x^2 - y^2$ and z^2 above these. The noncylindrical axial ligand, $L(H_2O)$, in **1** causes a small split in the xz ($1b_1$) and yz ($1b_2$) orbitals, but they still remain nearly degenerate, which indicates a triplet ground state for **1**. These two orbitals π interact with oxygen, in a destabilizing way:

$1b_2$ $1b_1$

The antibonding combinations of Fe d_π and O p_π orbitals have been used as an explanation for the instability of the ferryl complexes.[9] A slipping displacement of oxygen toward nitrogen (corresponding to an insertion of oxygen into the iron–nitrogen bond) reduces the antibonding character between iron and oxygen, and bonding between nitrogen and oxygen is increased, mainly through interaction of the p_x orbital of oxygen with an empty p_z orbital on nitrogen. The overlap population between iron and oxygen diminishes from 0.47 to 0.18 when going from **1** to **6**, whereas an increase from 0.00 to 0.65 between nitrogen and oxygen is observed. It should furthermore be pointed out that the overlap population between iron and the nitrogen, to which oxygen also is bound, in **6** goes from 0.41 in **1** to 0.29 in **6**, indicating that the iron–nitrogen bond is weakened by insertion of oxygen.

Oxo-iron porphyrins might be formed as shown in Scheme I, which in principle is a reaction between iron porphyrins and neutral oxygen. If we use this picture for the formation of oxo-iron porphyrins, we have an analogy to the carbene–iron porphyrins, where the carbene is inserted into the iron–nitrogen bond,[12] as carbene and oxygen are isoelectronic. The instability of oxo-iron porphyrins relative to the carbene analogue comes then from two major differences between oxygen and carbene: One difference is that oxygen has two p_π orbitals which can interact with Fe d_π orbitals while carbene has only one. The last two electrons in the oxygen case enter Fe d_π–O p_π antibonding orbital. The other is the difference in p-orbital energies. The p-orbital energy of oxygen is located much lower than the iron d-orbital energy, while the p-orbital energy of carbene lies very close to iron d. It might thus be expected from the second-order perturbation energy term that the interaction with carbene is more stabilizing than with oxygen, mainly because of the energy difference in the denominator.

Movement of the oxygen toward nitrogen will mix the iron d orbitals. Within the INDO framework the $x^2 - y^2$ orbitals mix with $-xz$ giving **8**, and the xy mix with yz giving **8A**. The shapes of these new orbitals are shown below.

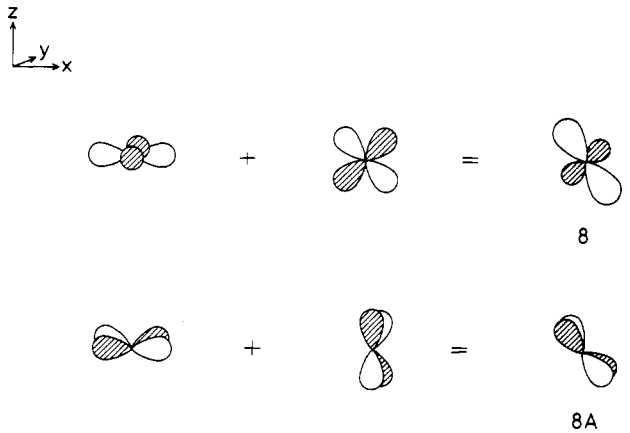

8

8A

Using extended Hückel calculations the z^2–xz mixing is dominant and the xy–zy less.

By changing the structure of oxo-iron porphyrins from a highly symmetric structure (**1**) to the structure with C_s symmetry (**6**), the electronic configuration of iron changes from d^4 – d^6-like.

The oxo-iron porphyrin with oxygen inserted into the iron–nitrogen bond (**6**) might then be a realistic alternative to the usually written structure, **1**.

The axial ligand $L(H_2O)$ in **6** seems to have stabilizing effect on the total energy of the oxo-iron porphyrin system. Calculation of the total energy of **6** without the axial ligand present gives a stabilization of about 6.5 eV, which is about 1.5 eV higher than with the ligand present.

It should also be noted that movement of the oxygen toward the carbon connecting the two pyrrole rings (equivalent to a motion of oxygen at 45° in the x–y plane (see plane in Figure 1)) destabilizes the system and leads to a less likely structure.

Mechanism for Stereoselective Epoxidation

Based on the INDO and extended Hückel calculations, the introduction of **6** leads to a new way of viewing this type of stereoselective epoxidation, as some iron d orbitals become available for an interaction with the alkene.[15] As a starting point for the mechanistic investigation, the following approach is proposed: The first step is an interaction of the alkene with the iron atom in **6** giving **9**. The next step is a displacement of the alkene toward the oxygen giving a three-membered transition state **9′**, which leads to the epoxide and the iron porphyrin (Scheme II).

Let us start with the frontier orbitals of oxo-iron porphyrin **6**, of which only the orbitals necessary for the analysis here are shown in Figure 2. The two unoccupied Fe d orbitals located at high

(14) The stability of **6** relative to **1** is probably exaggerated as INDO "loves" small rings.

Scheme II

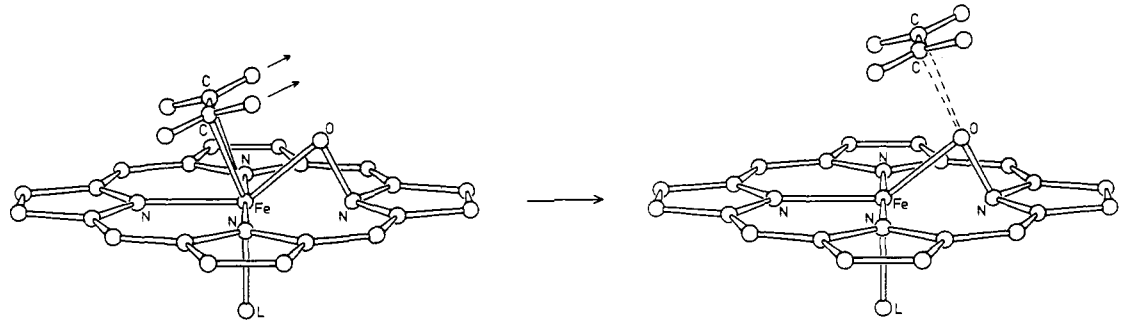

9 9'

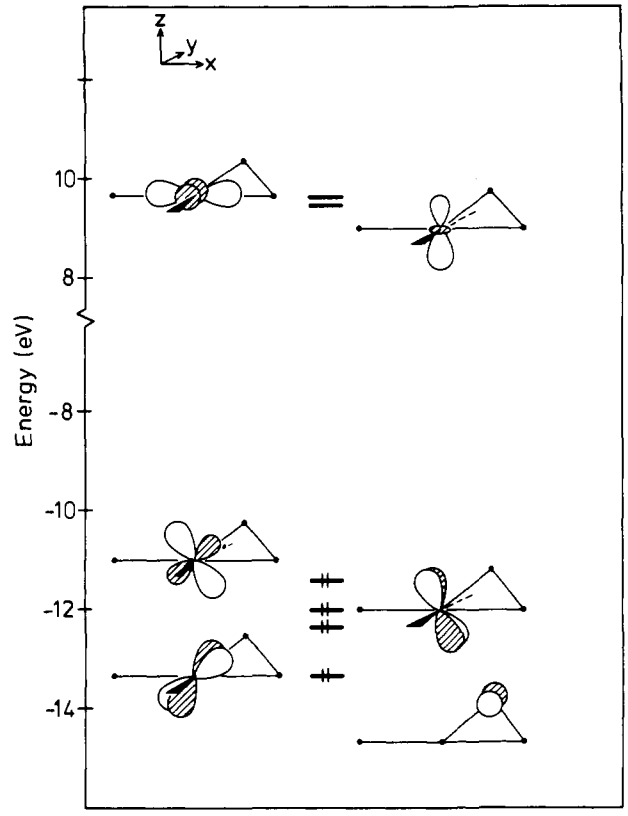

Figure 2. The INDO valence orbitals of **6** (only those related to the analysis presented here are shown).

energy are mainly $x^2 - y^2$ mixed in with a small part of z^2, and z^2 mixed with a small part of $x^2 - y^2$ and p_z. The mixing of z^2 and p_z orbitals is due to the interaction of the iron atom with the axial H_2O. Among the occupied orbitals we find the three remaining Fe d orbitals. The highest occupied orbital with dominant Fe character is located at about −11.5 eV appearing as $-xz$ mixed with $x^2 - y^2$, and the next two Fe d orbitals are a combination of xy and yz. About 1 eV below the last two Fe d orbitals we find one which is dominantly p_y orbital on O, and just right below the $p_x - p_y$ combination on oxygen is found. The orbitals calculated by the INDO program (shown in Figure 2) are delocalized to a greater extent than those calculated by the extended Hückel method (not shown here). Extended Hückel calculations give xz mixed with z^2 as HOMO located at −11.0 eV, yz mixed in with a small part of xy at −11.2 eV, and xy mixed in with a small part of yz at −12.1 eV. The LUMO is z^2 mixed with xz located at −9.2 eV; $x^2 - y^2$ is found at −6.3 eV. The oxygen p_y orbital energy is, using extended Hückel calculations, found about 2 eV lower than within the INDO model, and the p_x–p_z combination, just below.

Figure 3 shows the contour plot of the two empty Fe d orbitals, which are based on the extended Hückel calculations. The d character of the HOMO and second HOMO appears from Figure 3a,b; the xz mixed in with z^2 character is seen in Figure 3a and the yz character, in Figure 3b. Furthermore, the contour plots of LUMO and second LUMO also show the d character; Figure 3c shows the z^2 character and Figure 3d shows $x^2 - y^2$.

Figures 2 and 3 indicate that the possible interactions between an alkene and the iron d orbitals are between the ethylene π and the z^2 dominant orbital and between the ethylene π^* and the second highest occupied d orbital. The alkene can bind in two different ways to the iron atom, perpendicular to the iron–oxygen bond, **9**, or parallel to it, **10**.

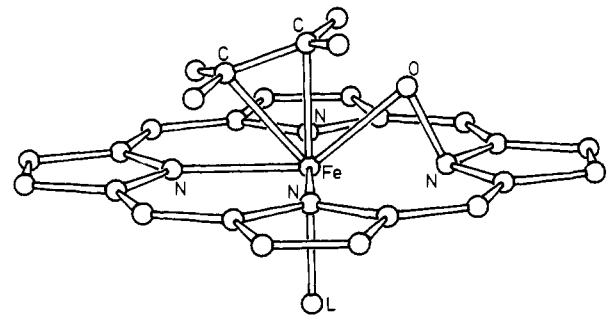

10

INDO as well as extended Hückel calculations for an ethylene complex give the preferred binding of the alkene to the iron in **6** as the conformation shown in **9**.[15-17] The iron–carbon bond length is calculated to be 2.2 Å and thus corresponds well with the one in $Fe(CO)_4C_2H_4$ (2.117 Å) determined by gas-phase electron diffraction.[18] The optimum angle for the oxo-iron porphyrin–alkene complex, **9**, has been found to be about 70°. A similar angle between the iron porphyrin plane and the center of the carbon–carbon double bond is found for **10**, but **9** was found to be more stable with a rotation barrier of about 10 kcal mol^{-1}. The preferred binding of the alkene in the perpendicular orientation relative to the iron–oxygen bond in **9** can be traced to the frontier orbitals: The ethylene acceptor orbital, π^*, antisymmetric with respect to the xz plane, is able to interact with the a″ occupied d orbital on iron located at −12.0 eV (Figure 2), whereas this type of interaction is not possible in **10**. With bond length between iron and carbon in the alkene at 2.10 Å and a binding angle of 70° between the iron porphyrin plane and the alkene, the distances from carbon and hydrogen (those nearest the iron porphyrin plane) to the iron porphyrin plane are 1.88 and 1.58 Å, respectively. It thus appears that the binding of trans alkenes to the iron atom, as shown in **9**, should be expected to be prevented when large trans

(15) See, e.g.: Wiekinson, G.; Stone, F. G. A.; Abel, E. W. *Comprehensive Organometallic Chemistry*; Pergamon Press: London, 1982; Vol. 4, p 377 for a discussion of alkene binding to iron compounds.

(16) Davis, M. I.; Speed, C. S. J. *Organomet. Chem.* **1970**, *21*, 401.

(17) (a) Hoffmann, R.; Albright, T. A.; Thorn, D. L. *Pure Appl. Chem.* **1978**, *50*, 1. (b) Albright, T. A.; Hoffmann, R.; Thibeault, J. C.; Thorn, D. L. *J. Am. Chem. Soc.* **1979**, *101*, 3801.

(18) A nearly similar mechanism has been suggested for epoxidation of alkenes using $[MO(O_2)_2$, M = Cr, Mo, W]: Jørgensen, K. A.; Hoffmann, R. *Acta Chem. Scand., Ser. B* **1986**, *40*, 411.

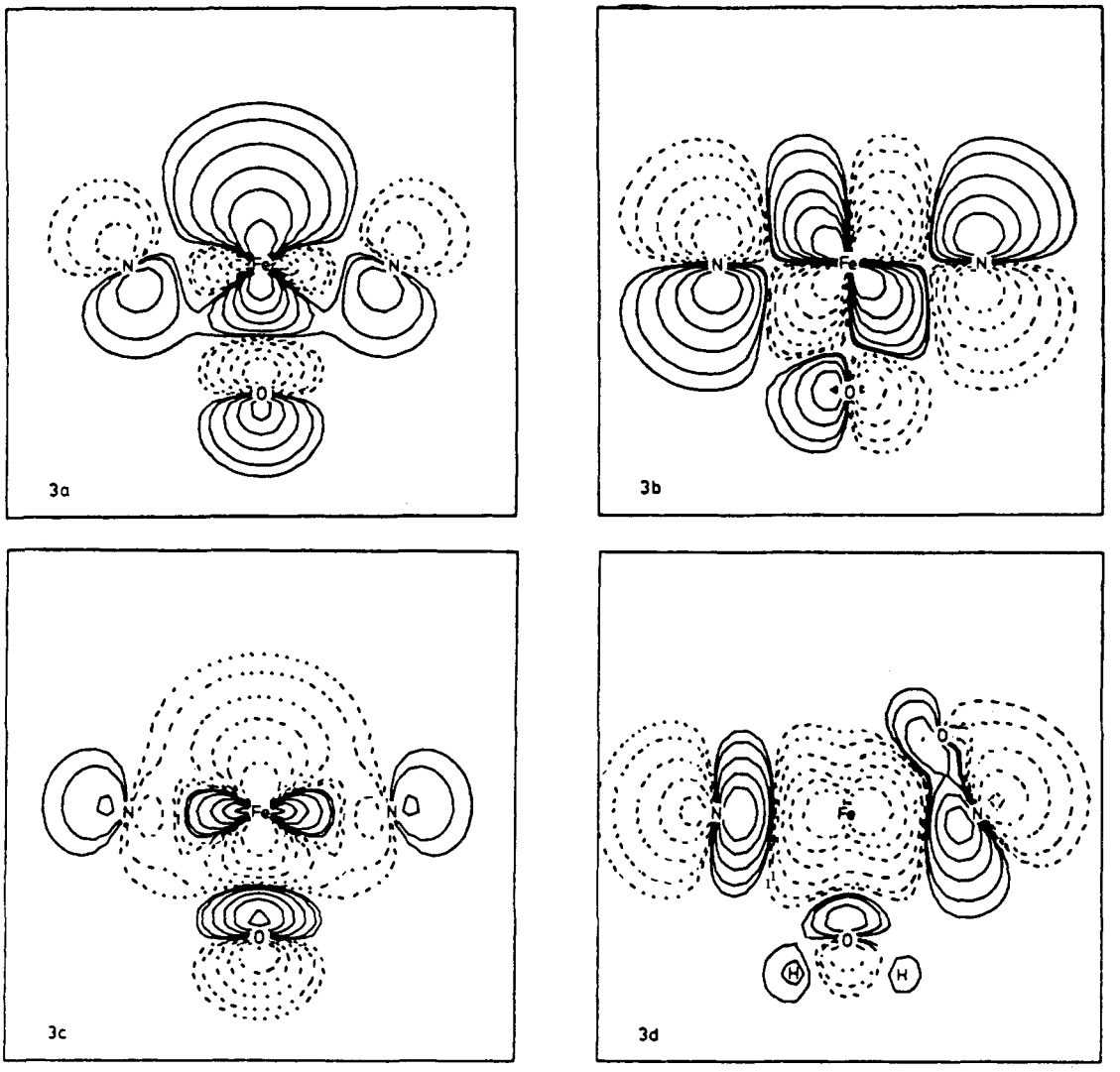

Figure 3. A plot of the valence orbitals (extended Hückel) of oxo-iron porphyrin. The contours of the levels of ψ are 0.2, 0.1, 0.055, 0.025, 0.01, and 0.005. The HOMO (3a), second HOMO (3b), and LUMO (3c) are plotted in the *yz* plane; the second LUMO is plotted (3d) in the *xz* plane.

Scheme III

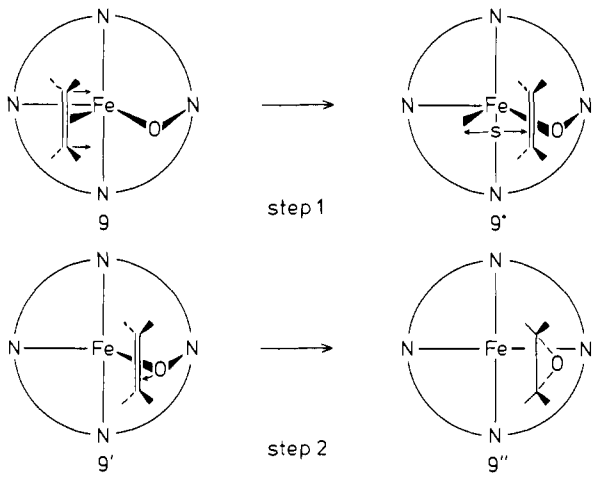

substituents are present, because of the steric repulsion between the alkene substituent and the iron porphyrin plane or bulky substituents in the 5α, 10α, 15α, and 20α positions in the porphyrin ring. Complex **10** can to some extent be viewed as a variation of geometry **3**, but it appears from both the experimental point of view as well as the theoretical to be less favorable.

Coupling of the alkene with the iron reduces the overlap population between iron and oxygen from 0.18 in **6** to −0.01 in **9**, indicating that no bond between iron and oxygen is present. The bond change allows us to compare the active oxygen transfer species in **9** with an *N*-oxide. Such an intermediate makes the similarity to the nickel analogue structure of **6** obvious, as these formed by the reaction of Ni(II) with the dianion of octaethylporphyrin *N*-oxide.[13]

Our studies of the preferred orientation of an alkene in the coordination sphere of the iron atom leads naturally to the suggested epoxidation mechanism (Scheme II). With **9** as the preferred conformation of the oxo-iron porphyrin–alkene complex, it appears that the frontier orbitals of ethylene and oxygen are set up for an interaction, **11**. The alkene π^* orbital, antisymmetric

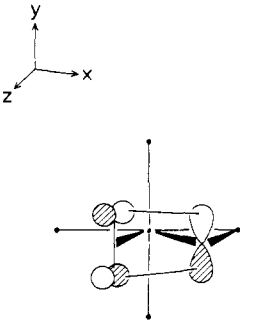

11

with respect to the *xz* plane, has then the right symmetry to

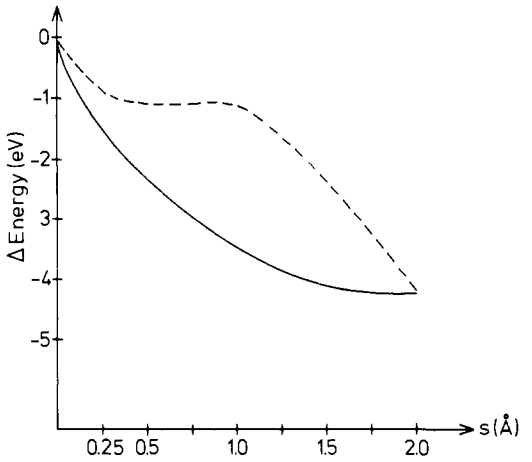

Figure 4. The change in total energy for step 1 as a function of the slipping distance *s*. The full line represents INDO calculations and the dotted line extended Hückel.

interact with the lone-pair electrons on oxygen located in the p_y orbital (Figure 2), which also is antisymmetric with respect to the same plane. This obviously leads to the suggested mechanism.[18] A slipping movement of the alkene of this type will lead to a three-membered transition state.

For further clarification of the mechanism shown in Scheme II, it will be divided into two steps as shown in Scheme III. The first step is a slipping motion of the alkene, in a perpendicular orientation relative to the iron–oxygen plane, toward oxygen at a distance of 2 Å from the iron–oxygen bond. The second step, movement of oxygen, takes place with fixed iron–nitrogen–oxygen angle, as an increase of the nitrogen–oxygen distance, which leads to **9″**.

The change in total energy for the system in the first step as a function of the displacement, *s*, is shown in Figure 4. The full line is the change in total energy from INDO calculations while the dashed line is the same from the extended Hückel model.

It is shown in Figure 4 that the total energy for the oxo-iron porphyrin–alkene complex decreases with the displacement *s*. The curves, which represent the relative change in total energy calculated by the two different procedures, show the same general trend, as both INDO and extended Hückel indicate that the system is stabilized by −4.2 eV, when the alkene is in front of the oxygen. INDO calculations indicate that the total energy decreases monotonically as a function of the slipping distance *s*, whereas extended Hückel calculations exhibit a shoulder at about 1 Å. The decrease in energy for the system can be traced to an increased overlap between iron and oxygen. When the alkene is in front of the oxygen, the interaction between the alkene π^* and oxgen p_y, as depicted in **11**, becomes stabilizing and then contributes in lowering the energy of the system.

The change in total energy for the system for step 2, movement of the oxygen toward the alkene, is depicted in Figure 5. Figure 5a shows the result of the INDO calculations. Two sets of calculations are shown, one (dashed line) with the starting point being the alkene slipped by a moderate amount, 1.0 Å, the other slipped so it is in front of the oxygen (2.0 Å). Figure 5b shows the extended Hückel calculations at the same geometries as those used in Figure 5a.

The results of the calculation of the change in total energy presented in Figure 5 show nearly the same pattern; the INDO calculations (Figure 5a) give a destabilization of the system for a moderate displacement of the alkene (1.0 Å, the dashed line), and similar results are obtained by extended Hückel calculations (Figure 5b, dashed line). For a 2-Å displacement of the alkene, both INDO and extended Hückel calculations show a transition state at a nitrogen–oxygen bond extension of about 0.35 Å, which corresponds to a carbon–oxygen distance at about 2.0 Å which is in agreement with the distance found in the theoretical studies of peracid epoxidation.[19] After the transition state has been

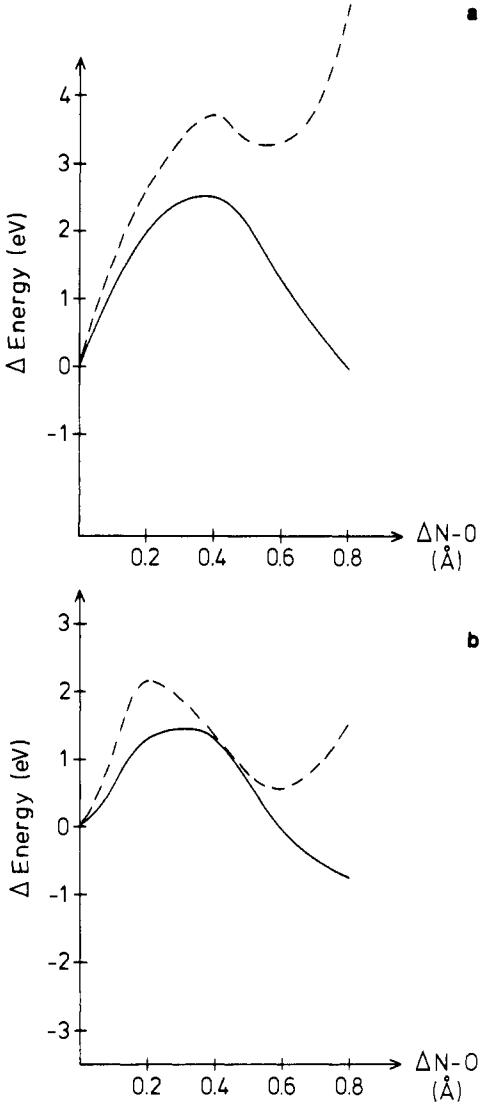

Figure 5. (a) The change in total energy (INDO calculations) for step 2 as a function of extension of nitrogen–oxygen distance. The full line designates when the alkene is slipped by a moderate amount, 1.0 Å, the other slipped 2 Å. (b) The same as in Figure 5a, but with extended Hückel calculations.

reached, a decrease in total energy is found, caused by formation of a carbon–oxygen bond which stabilizes the complex.

Summarizing the results for steps 1 and 2 (Scheme III), both sets of calculations give a stabilization of the system when the alkene moves from iron to oxygen. It is worth mentioning that both INDO calculations, which have a total energy expression, and extended Hückel calculations, where the total energy is represented by a sum of orbital energies, give the same stabilization. For the second step the INDO and extended Hückel procedures give nearly similar transition states followed by a decrease in energy leading to **9″**. Calculation of a total energy potential surface for the alkene displacement and nitrogen–oxygen bond extension (not shown here) gives the important places as those discussed above.

From **6** there might also be a second approach by which the stereoselective epoxidation of alkenes can take place, the alkene interacts here directly with the oxygen as shown in **12**. This is

(19) For some calculated bond lengths between carbon and oxygen in peroxy acid epoxidation reactions, see, e.g.: (a) Bach, R. D.; Willis, C. L.; Domagala, P. *Prog. Theor. Org. Chem.* **1977**, *2*, 221. (b) Azman, A.; Borstnik, B.; Plesnicar, B. *J. Org. Chem.* **1969**, *34*, 971. (c) Yonezawa, T.; Kato, H.; Yamamoto, O. *Bull. Chem. Soc. Jpn.* **1967**, *40*, 307. (d) Plesnicar, B.; Taserski, M.; Azman, A. *J. Am. Chem. Soc.* **1978**, *100*, 743.

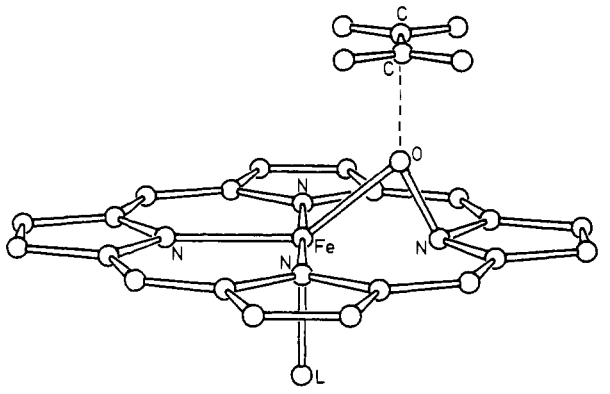

12

a type of variant of the mechanism shown in Scheme II; the only difference is that the alkene here "comes down" from the top and is thus not complexed by the iron as in the other mechanism. This mechanism will also to some extent cause preference of epoxidation of cis alkenes rather than trans alkenes, as the trans substituents will interact repulsively when large bulky substituents are located in the 5α, 10β, 15α, and 20β positions in the porphyrin ring. A detailed investigation of the change in total energy for this particular oxo-iron porphyrin–alkene system (not presented here) using this mechanistic approach gives higher activation energy and less stable intermediates compared with the mechanism outlined in Schemes II and III.

The mechanism for the stereoselective epoxidation of cis alkenes presented here agrees well with the experimental observations. *A very recent* paper by Groves[20] gives further support to the first step (the coordination of the alkene to iron **9**), presented here as the first step in the reaction. In this paper[20] it was stated that visible spectral changes were observed after the addition of alkene to iron porphyrin, indicating that a stable intermediate was formed prior to the epoxidation product. It has furthermore been found that the reaction of oxo-iron porphyrin with substituted styrenes correlated with the Hammett σ^+ with large negative σ^+ (−1.9). This negative Hammett is consistent with an initial electron-transfer process between the oxo-iron porphyrin and the substrate,[20] which according to the MO picture of the oxo-iron porphyrin presented in Figure 2 does not seem unrealistic. The negative Hammett value does then correlate with a complexation of the alkene to the iron center. The next step in the epoxidation mechanism, the interaction of the alkene with the oxygen, can also be compared with Bartlett's widely accepted mechanism for the epoxidation of alkenes by peroxy acids,[21] which recently has received theoretical support.[19] The oxygen which is transferred from the oxo-iron porphyrin to the alkene can to some extent be compared with the epoxidizing oxygen in peroxo acids as well as the oxygen in transition metal peroxo compounds as, e.g., $MoO(O_2)_2$ **13**[22] and (dipic)VO(OO-*t*-Bu)·H_2O (**14**);[23] the only difference is that the oxygen in oxo-iron porphyrin is bound to a nitrogen rather than an oxygen.

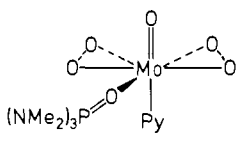

13

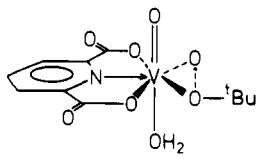

14

Let us also try to compare the mechanism suggested here with the catalytic epoxidation of alkenes with (salen)Cr^{III},[24] where the geometry of oxochromium(V) cation **15** is known.[24b] **15** is a high-symmetry structure, which can be compared with **1**. The catalytic epoxidation of various alkenes with iodosobenzene and **15** (= oxo-oxygen) as catalyst shows no stereoselectivity, as both trans and cis alkenes are epoxidized in about equal amounts. Two intermediates have been discussed.[24a] One is a four-membered chromium–oxygen–carbon–carbon ring and the other can be compared with 2 which is a close relative to the activated complex based on the concept of least motion for the rate-limiting step. With this in mind, the mechanism for which it has been advocated here seems not unrealistic.

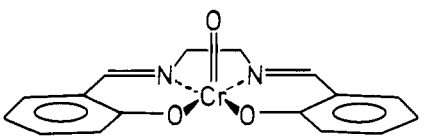

15

Table I. Parameters Used in INDO Calculations

	orbital	exponents[a] ζ_1	ζ_2	ζ_3
H	1s	1.20	1.20	
C	2s	1.625	1.625	
	2p	1.625	1.625	
N	2s	1.95	1.95	
	2p	1.95	1.95	
O	2s	2.275	2.275	
	2p	2.275	2.275	
Fe	4s	1.37	1.37	
	4p	1.37	1.37	
	3d	3.3829	6.0683 (0.4038)	2.6184 (0.7198)

[a] Coefficients and exponents in ζ expansion.

Table II. Parameters Used in Extended Hückel Calculations

	orbital	H_{ii}	a exponents ζ_2	ζ_2
H	1s	−13.6	1.3	
C	2s	−21.4	1.625	
	2p	−11.4	1.625	
O	2s	−32.3	2.275	
	2p	−14.8	2.275	
N	2s	−26.0	1.875	
	2p	−13.4	1.65	
Fe	4s	−9.10	1.90	
	4p	−5.32	1.90	
	3d	−12.60	5.35 (0.53659)	1.80 (0.66779)

[a] Coefficients and exponents in a ζ expansion.

Summary

This paper tries to give a coherent theoretical model for the stereoselective epoxidation of alkenes by oxo-iron porphyrins. It has been found that the structure of oxo-iron porphyrin is one in which the oxygen is inserted into the iron–nitrogen bond. The calculated iron–oxygen and nitrogen–oxygen bond lengths are in good agreement with those recently found by X-ray crystallography investigation of the nickel analogue. It is suggested that the first step in the reaction is a binding of the alkene to the iron center in an orientation in which the alkene is perpendicular to the iron–oxygen bond. Cis alkenes have a preference for coordination to thee iron atom, as steric substituents in the trans will interact repulsively with the porphyrin ring or substituents in the 5α, 10α, 15αa, and 20α positions in the porphyrin ring. This

(20) Groves, J. T.; Watanabe, Y. *J. Am. Chem. Soc.* **1986**, *108*, 507.
(21) Bartlett, P. D. *Rec. Chem. Prog.* **1957**, *18*, 111.
(22) See, e.g.: Le Carpentier, J.-M.; Mitschler, A.; Weiss, R. *Acta Crystallogr., Sect. B, Struct. Sci.* **1972**, *28*, 1278.
(23) Minoun, H.; Chaumette, P.; Mignard, M.; Sausinne, L. *Nouv. J. Chim.* **1983**, *7*, 467.
(24) (a) Samsel, E. G.; Srinivasan, K.; Kochi, J. K. *J. Am. Chem. Soc.* **1985**, *107*, 7606. (b) Srinivasan, K.; Kochi, J. K. *Inorg. Chem.* **1985**, *24*, 4671.

complex is supported by very recent spectral studies of the change to absorbance after the addition of alkene to oxo-iron porphyrin. From this complex the epoxide is formed by a slipping displacement of the alkene toward the oxygen, which leads to a favorable interaction between the π^* of the alkene and the lone pair on the oxygen.

Acknowledgment. Thanks are expressed to Professors Kurt Torssell and Jan Linderberg for fruitful discussions and to Dr. Peter Swanstrøm for setting up the programs. Thanks are also expressed to a referee for comments about the INDO calculations.

Appendix

All calculations were performed using transition metal INDO,[7] CNDO,[7] and extended Hückel[8] calculations. The parameters used in the INDO and CNDO calculations are given in Table I and in extended Hückel calculations in Table II.

Registry No. 6, 105930-44-7.

Ab Initio Theoretical Studies of Dihydrogen Coordination vs. Oxidative Addition of H_2 to Five-Coordinate Tungsten Complexes

P. Jeffrey Hay

Contribution from Theoretical Division, Los Alamos National Laboratory, Los Alamos, New Mexico 87545. *Received June 2, 1986*

Abstract: Various modes of H_2 bonding to d^6 metal complexes are investigated using ab initio electronic wave functions and relativistic effective core potentials. The novel η^2 form in $W(CO)_3(PR_3)_2(H_2)$ complexes, in which the H–H bond remains intact, is contrasted with seven-coordinate dihydride WL_5H_2 complexes, in which oxidative addition to the metal center has occurred. The influence of the electronic properties of the ligands in the relative stability of these forms is also discussed.

I. Introduction

Several compounds of a new class of dihydrogen metal complexes have recently been synthesized[1,2] in which the H–H bond remains essentially intact, in contrast to the traditional situation in oxidative addition[3] wherein the H–H bond is cleaved with the formation of two metal–hydrogen bonds or the analogous case of C–H activation.[4] In the dihydrogen compounds first characterized by Kubas et al.,[1a] the H_2 is bonded to five-coordinate d^6 metal center in $W(CO)_3(PR_3)_2(H_2)$ and its Mo analogue. The factors governing the stability of these dihydrogen species relative to their more familiar dihydride forms are being explored experimentally[1,2] and theoretically.[5,6]

In this study we present the first ab initio theoretical study of these species. We will analyze the relative stability of the two forms—the six-coordinate dihydrogen and the seven-coordinate dihydride—and we will explore the important role the ligand can play in stabilizing one form or the other. In particular, we present results of ab initio calculations on model complexes $W(CO)_3(PR_3)_2(H_2)$ and $W(PH_3)_5(H_2)$ where the effects of replacing the strongly π-accepting CO ligands by PR_3 groups can be probed. Using ab initio approaches, in contrast to semiempirical methods for metal complexes, one can optimize the bond lengths and other geometrical parameters and then compare the relative energies of the various geometrical forms of the molecule. The results of these studies are presented in the next sections, and the details of the calculation appear at the end.

II. Bonding of H_2 to WL_5 Fragments

A. $W(CO)_3(PH_3)_2(H_2)$ Complexes. Structures **1–3** exemplify the modes of H_2 bonding to a $W(CO)_3(PH_3)_2$ fragment: two sideways bonded (η^2-coordinated) forms (**1** and **2**) and the end-on

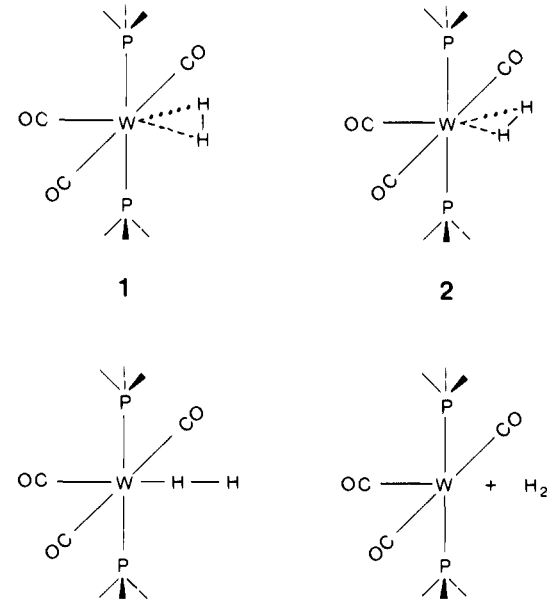

bonded (η^2-coordinated) form (**3**). Using a rigid $W(CO)_3(PH_3)_2$ fragment, the geometries of these three forms of H_2 coordination

(1) (a) Kubas, G. J; Ryan, R. R.; Swanson, B. I.; Vergamini, P. J.; Wasserman, H. *J. Am. Chem. Soc.* **1984**, *106*, 451. (b) Kubas, G. J.; Ryan, R. R; Wrobleski, D. *Ibid.* **1986**, *108*, 1339. (c) Wasserman, H. J.; Kubas, G. J. Ryan, R. R. *Ibid.* **1986**, *108*, 2294. (d) Kubas, G. J; Unkefer, G. J.; Swanson, B. I.; Fukishima, E. *Ibid.* **1986**, *108*, 7000.

(2) (a) Sweany, R. L. *J. Am. Chem. Soc.* **1985**, *107*, 2374. (b) Upmacis, R. K.; Gadd, G. E.; Poliakoff, M.; Simpson, M. B.; Turner, J. J.; Whyman, R. Simpson, A. F., *J. Chem. Soc., Chem. Commun.* **1985**, 27. (c) Church, S. P.; Grevels, F.-W.; Hermann, H.; Schaffner, K. *Ibid.* **1985**, 30. (d) Crabtree, R. H.; Lavin, M. *Ibid.* **1985**, 794, 1661. (e) Morris, R. H.; Sawyer, J. F.; Shiralian, M.; Zublowski, J. D. *J. Am. Chem. Soc.* **1985**, *107*, 5581. (f) Gadd, G. E.; Upmacis, R. K.; Poliakoff, M.; Turner, J. J. *Ibid.* **1986**, *108*, 2547. (g) Ozin, G. A.; Garcia-Prieto, J. *Ibid.* **1986**, *108*, 3099. (h) Upmacis, R. K; Poliakoff, M.; Turner, J. J. *Ibid.* **1986**, *108*, 3645. (i) Clark, H. C.; Hampden Smith, M. J. *Ibid.* **1986**, *108*, 3829. (j) Crabtree, R. H.; Lavin, M.; Bonneviot, L. J. *Ibid.* **1986**, *108*, 4032. (k) Sweany, R. L. *Organometallics* **1986**, *5*, 387. (l) Conroy-Lewis, F. M.; Simpson, S. J. *J. Chem. Soc., Chem. Commun.* **1986**, 506. (m) Crabtree, R. H.; Hamilton, D. G. *J. Am. Chem. Soc.* **1986**, *108*, 3124.

(3) (a) Collman, J. P. *Acc. Chem. Res.* **1968**, *1*, 136. (b) Vaska, L. *Ibid.* **1970**, *3*, 386. (c) James, B. R. *Homogeneous Hydrogenation*; Wiley: New York, 1973.

(4) For leading references on C–H activation, see, for example: Crabtree, R. *Chem. Rev.* **1985**, *85*, 245.

(5) Hay, P. J. *Chem. Phys. Lett.* **1984**, *103*, 466.

(6) (a) Saillard, J. Y.; Hoffmann, R. *J. Am. Chem. Soc.* **1984**, *106*, 2006. (b) Bagatur'yants, A. A.; Anikin, N. A.; Zhidomirov, G. M.; Kazanskii, V. B. *Zh. Fiz. Khim.* **1981**, 55, 2035. (c) Hoffmann, R.; Beier, B. F.; Muetterties, E. L.; Rossi, A. R. *Inorg. Chem.* **1977**, *16*, 511. (d) Sevin, A.; *Nouv. J. Chim.* **1981**, *5*, 233. (e) Sevin, A.; Chaquin, P. *Ibid.* **1983**, *7*, 353.

0002-7863/87/1509-0705$01.50/0